

Rotational excitation of methylidyne (CH^+) by a helium atom at high temperature

K. Hammami¹, L. C. Owono Owono^{2,3}, and P. Stäuber⁴

¹ Laboratoire de Spectroscopie Atomique Moléculaire et Applications, Département de Physique, Faculté des Sciences, Université Tunis El Manar, Campus Universitaire, 1060 Tunis, Tunisia
e-mail: hammami283@yahoo.fr

² Department of Physics, Advanced Teachers Training College, University of Yaounde I, P.O. Box 47, Yaounde, Cameroon

³ Centre for Atomic Molecular Physics and Quantum Optics, Faculty of Science, University of Douala, P.O. Box 8580, Douala, Cameroon

⁴ Institute for Astronomy, ETH Zurich, 8093 Zurich, Switzerland

Received March 25, 2009; accepted March 16, 1997

ABSTRACT

Context. The *Herschel Space Observatory* with its high-resolution instrument HIFI on board will observe the CH^+ $1 \rightarrow 0$ and $2 \rightarrow 1$ rotational transitions in a wide range of gas temperatures up to 1000 K. Collisional parameters for such temperatures are thus welcome.

Aims. We aim to obtain accurate rate coefficients for the collisional excitation of CH^+ by He for high gas temperatures.

Methods. The *ab initio coupled-cluster* [CCSD(T)] approximation was used to compute the interaction potential energy. Cross sections are then derived in the close coupling (CC) approach and rate coefficients inferred by averaging these cross sections over a Maxwell-Boltzmann distribution of kinetic energies.

Results. Cross sections are calculated up to $10\,000\text{ cm}^{-1}$ for J ranging from 0 to 10. Rate coefficients are obtained at high temperatures up to 2000 K.

Key words. ISM: molecules – molecular data – molecular processes – astrochemistry – radiative transfer

1. Introduction

The molecular ion CH^+ ($X^1\Sigma^+$) is most commonly observed from the ground in the visible in absorption lines against nearby bright stars. The lowest rotational transitions in the submillimeter and far-infrared band are blocked from the earth's atmosphere and therefore difficult to observe with ground-based telescopes. A tentative detection of the $J = 1 \rightarrow 0$ transition of the isotope $^{13}\text{CH}^+$ has been reported recently by Falgarone et al. (2005). Cernicharo et al. (1997) reported the first emission lines of the $J = 2 \rightarrow 1$, $3 \rightarrow 2$ and $4 \rightarrow 3$ rotational transitions detected with the *Infrared Space Observatory*.

Although CH^+ has been observed frequently in the ISM over the past few decades, its abundance is still an enigma. Chemical models persistently fail to reproduce the large abundances, as it is not yet clear, what the main source for CH^+ is (Black et al. 1978; Black 1998; Nehmé et al. 2008). The highly endothermic reaction $\text{C}^+ + \text{H}_2 \rightarrow \text{CH}^+ + \text{H}$ ($-\Delta E/k = 4640\text{ K}$) is proposed as the most efficient route to CH^+ . Besides high gas temperatures, an important part of the energy needed to activate this reaction may come from vibrationally excited H_2 (Sternberg & Dalgarno 1995). Since CH^+ is also abundantly found in the cold neutral medium (CNM), this reaction may not be fast enough though to compete with the destruction reactions. Attempts to resolve this puzzle continue (Joulain et al. 1998; Godard et al. 2009). A thorough understanding of the CH^+ abundance is important since it provides information about physical gas properties such as temperature and fraction of ionization. Furthermore, CH^+ is a fundamental building block for more complex molecules and a relevant coolant in hot and dense interstellar gas.

Related to the problem to model observed CH^+ abundances is the uncertainty in the excitation mechanism. The CH^+ is likely to be destroyed rather than excited in collisions with hydrogen and electrons - the most abundant species. In addition, the excitation of CH^+ is found to be sensitive to the dust continuum background of the CH^+ emitting source (Black 1998). To model the CH^+ abundance, the chemical reactions and radiative transfer equations may therefore need to be solved simultaneously. However, excitation calculations require accurate collisional rate coefficients.

Observations with the *Herschel Space Observatory* may shed some light on these problems. The high spectral resolution instrument HIFI onboard the satellite will observe the $J = 1 \rightarrow 0$ and $J = 2 \rightarrow 1$ rotational transitions in a wide range of interstellar gas from the diffuse ISM to dense and hot star-forming regions. PACS, another instrument for *Herschel*, will cover the CH^+ transitions with $J_{\text{up}} = 2-6$. Since the CH^+ abundance is sensitive to far-ultraviolet (FUV) photons and X-rays (Sternberg & Dalgarno 1995; Stäuber et al. 2004, 2005), it will be searched for in typical photo-dissociation regions (PDRs) and X-ray dominated regions (XDRs). The gas temperature in such areas can easily reach a few 1000 K (Tielens & Hollenbach 1985; Maloney et al. 1996). Collisional rate coefficients are therefore needed for a large range of gas temperatures and upper energy levels in order to interpret the observations properly.

The aim of this paper is to obtain accurate rate coefficients for the collisional excitation of CH^+ at high temperatures. As it is far more difficult to determine rate coefficients for excitation with H_2 , we focus on the rotational excitation by He, another

major gas component. This study is thus an extension of an earlier published paper, where coefficients for temperatures up to 200 K were presented (Hammami et al. 2008).

2. Potential energy surface

Recently, we have computed the interaction PES for the CH⁺(X¹Σ⁺) – He(¹S) van der Waals system using the rigid rotor approximation and the Jacobi coordinate system in which r is the CH⁺ internuclear distance, R the distance from the center of mass (c.m.) of CH⁺ to the He atom, and θ the angle between the two distance vectors (Hammami et al. 2008). The collinear CH⁺...He geometry corresponds to $\theta = 0^\circ$ while the CH⁺ bond distance was frozen at its value at the experimental equilibrium geometry of the ground X¹Σ⁺ state, i.e., $r = r_e = 2.1371$ Bohr (Huber & Herzberg 1979). Computations were carried out at the CCSD(T) level as it is implemented by Knowles et al. (1993, 2000) in the MOLPRO molecular package (Werner et al. 2002). All our calculations were performed with the augmented correlation consistent valence quadruple zeta (aVQZ) basis set of Woon & Dunning (1994) for all atoms. The (3s3p2d1f) set of bond functions defined by Tao & Pan (1992) are added and placed at mid-distance between the c.m. of CH⁺ and He.

The basis set superposition errors (BSSE) was corrected at all geometries following the Boys & Bernardi (1970) counterpoise procedure. Our PES has a global minimum of 537 cm⁻¹ at $R = 4.05$ Bohr and $\theta = 84^\circ$. This value is consistent with that obtained by Stoecklin & Voronin (2008) with the BCCD(T) method and a aug-cc-pVQZ basis set, i.e., 513 cm⁻¹ at $R = 4.1$ Bohr and $\theta = 86^\circ$. Indeed, our well depth is lower than their value.

To perform the dynamical calculations, the basic inputs required by the MOLSCAT package (Hutson & Green 1994) were obtained by expanding the interaction potential in terms of Legendre polynomials as

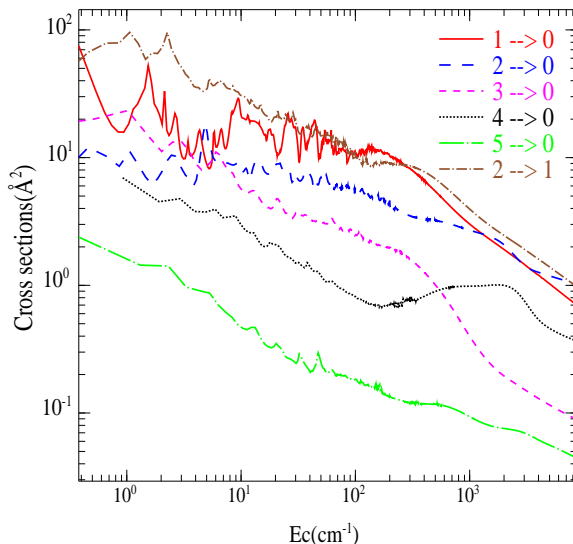
$$V(r = r_e, R, \theta) = \sum_{\lambda} V_{\lambda}(R) P_{\lambda}(\cos \theta). \quad (1)$$

The calculated surface is well reproduced by the analytical potential over the entire grid of used coordinate points. The standard deviation between the analytical and the calculated surface remains below 1.0%. Further details concerning calculations related to the interaction potential can be found in the paper by Hammami et al. (2008).

3. Cross sections

The quantum mechanical close coupling approach (Arthurs & Dalgarno 1960) implemented in the MOLSCAT code was used to calculate state to state rotational integral cross sections for values of J ranging from 0 to 10, and a total energy up to 10 000 cm⁻¹. The energy range was carefully spanned in order to account for resonances. The incremental steps were chosen as follows: From 0 to 50 cm⁻¹, they were set to 0.1 cm⁻¹, from 50 cm⁻¹ to 100 cm⁻¹ to 0.2 cm⁻¹, from 100 cm⁻¹ to 200 cm⁻¹ to 0.5 cm⁻¹, from 200 cm⁻¹ to 1200 cm⁻¹ to 1 cm⁻¹, from 1200 cm⁻¹ to 1400 cm⁻¹ to 2 cm⁻¹, from 1400 cm⁻¹ to 1500 cm⁻¹ to 5 cm⁻¹, from 1500 cm⁻¹ to 2000 cm⁻¹ to 10 cm⁻¹, from 2000 cm⁻¹ to 2500 cm⁻¹ to 25 cm⁻¹, from 2500 cm⁻¹ to 3000 cm⁻¹ to 50 cm⁻¹, from 3000 cm⁻¹ to 5000 cm⁻¹ to 100 cm⁻¹, and finally from 5000 cm⁻¹ to 10 000 cm⁻¹ to 200 cm⁻¹. To include all open channels and some closed channels, we have set $J_{max} = 15$ for $E \leq 1000$ cm⁻¹, and

Fig. 1. Deexcitation cross sections of CH⁺ by collision with He as a function of the kinetic energy.



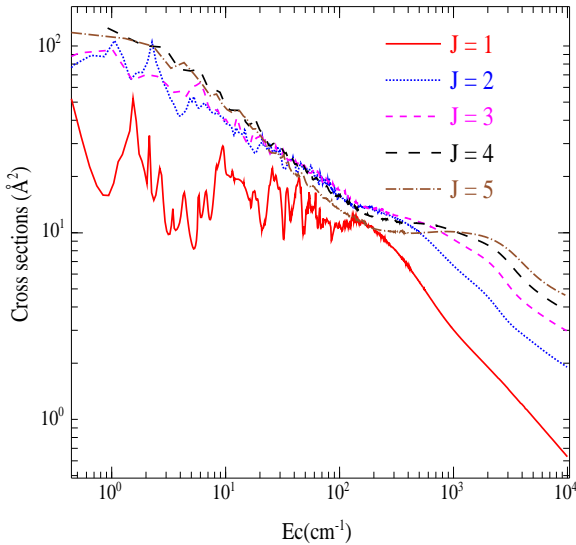
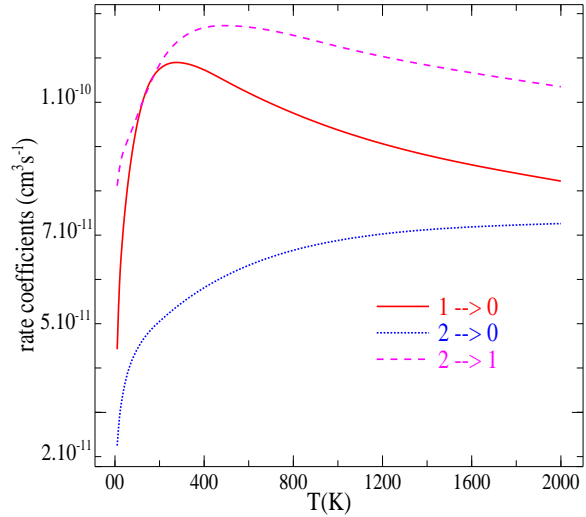
$J_{max} = 17$ for $E > 1000$ cm⁻¹. This corresponds to a rotational basis set of adequate size for a good accuracy in the calculated cross sections. The input parameters required by MOLSCAT are displayed in Table 1. These parameters were fixed after we have performed some tests to ensure the convergence of cross sections for energies up to 10 000 cm⁻¹. The coupled equations were conveniently solved using the propagator of Manolopoulos (1986).

Figure 1 presents the energy variation of the CH⁺ – He collisional deexcitation cross sections for the transitions $J \rightarrow 0$, for $J = 1 - 5$ and the transition $2 \rightarrow 1$. Up to almost 600 cm⁻¹, resonances can be seen in the cross sections. These are due to the global minimum located at 4.05 Bohr and whose well depth is ~ 537 cm⁻¹. As one can also see from the figure, the cross sections for the transition $1 \rightarrow 0$ are larger than those with $J > 1 \rightarrow 0$ almost over the entire range of energies. Some exceptions occur with the transition $2 \rightarrow 0$ for which cross sections are slightly larger around 5 cm⁻¹ and for $E_C \gtrsim 1000$ cm⁻¹. It is also obvious from the figure that the cross sections for the transition $2 \rightarrow 1$ are larger than those of the other transitions plotted but remain of similar magnitude as those of the transition $1 \rightarrow 0$ with increasing energy. Turning our attention to Fig. 2, it can be seen that our total cross sections are consistent both in shape and magnitude with the quenching cross sections calculated by Stoecklin & Voronin (2008) for energies lower than 1000 cm⁻¹.

An analysis of the excitation cross sections has been carried out by Hammami et al. (2008). It was pointed out in that for energies lower than 600 cm⁻¹, the cross sections for the transition $0 \rightarrow 1$ are larger than those for $0 \rightarrow 2$ while for energies greater than that, the converse holds. Similar observations were also made for the transition $1 \rightarrow 2$ and $0 \rightarrow 2$ for an energy of ~ 150 cm⁻¹. Indeed, for energies greater than that value, the transition $1 \rightarrow 2$ is less favored (see also Hammami et al. 2008). It should be noticed that there is a propensity towards ΔJ even parity transitions for almost the entire range of energy.

Table 1. MOLSCAT parameters used in the present calculations. Be and De are from Huber & Herzberg (1979).

INTFLG=6	STEPS=30	OTOL=0.01	DTOL=0.1
Be=14.1776 cm ⁻¹	De=0.0014 cm ⁻¹	JMAX=17	RMIN=3 Bohr, RMAX=50 Bohr

Fig. 2. Rotational quenching cross sections of CH⁺ by collision with He as a function of the kinetic energy.**Fig. 3.** Calculated downward rate coefficients for selected transitions as a function of the kinetic temperature.

4. Collisional rates

Downward rate coefficients are obtained by averaging the cross sections $\sigma_{J \rightarrow J'}$ over a Maxwell-Boltzmann distribution of kinetic energies,

$$q_{J \rightarrow J'}(T) = \left(\frac{8\beta^3}{\pi\mu} \right) \int_0^\infty E_C \sigma_{J \rightarrow J'}(E) e^{-\beta E_C} dE_C, \quad (2)$$

where T is the kinetic temperature, $\mu = 3.06139$ a.u. is the reduced mass of the CH⁺ – He collision partners, $\beta = \frac{1}{k_B T}$ (k_B is the Boltzmann constant) and $E_C = E - E_J$ is the relative kinetic energy. Table 2 displays the results at selected temperatures. Additional numbers may be obtained upon request to the authors. Figure 3 illustrates the variation of $q_{J \rightarrow J'}(T)$ with the kinetic temperature. The general trends observed earlier by Hammami et al. (2008) for these numbers at low temperature remain. As one can see from the figure, the magnitude of the rate coefficients for the transition $2 \rightarrow 1$ dominates followed by the $1 \rightarrow 0$ which is dominant over $2 \rightarrow 0$.

5. Summary

Using a previously computed PES (Hammami et al. 2008), we have obtained results of a quantum mechanical close coupling calculation of integral cross sections for transitions between the lower rotational levels of CH⁺ induced by collisions with He. The cross sections were averaged over a Maxwell-Boltzmann distribution of kinetic energies to determine downward rate coefficients. The kinetic temperature spans a wide range of values up

to 2000 K. The spectroscopic parameters obtained at high temperature exhibit the general trends for such quantities. The rate coefficients will help to understand and interpret astrophysical observations in connection with the Herschel Space Observatory mission.

Acknowledgements. Author LCOO acknowledges with thanks the financial support of the Abdus Salam International Centre for Theoretical Physics, Office of External Activities (ICTP-OEA) under NET45 Programme.

References

- Arthurs, A. M. & Dalgarno, A. 1960, Royal Society of London Proceedings Series A, 256, 540
- Black, J. H. 1998, in Chemistry and Physics of Molecules and Grains in Space. Faraday Discussions No. 109, 257–+
- Black, J. H., Hartquist, T. W., & Dalgarno, A. 1978, ApJ, 224, 448
- Boys, S. F. & Bernardi, F. 1970, Molecular Physics, 19, 553
- Cernicharo, J., Liu, X.-W., Gonzalez-Alfonso, E., et al. 1997, ApJ, 483, L65+
- Falgarone, E., Phillips, T. G., & Pearson, J. C. 2005, ApJ, 634, L149
- Godard, B., Falgarone, E., & Pineau Des Forêts, G. 2009, A&A, 495, 847
- Hammami, K., Owono Owono, L. C., Jaidane, N., & Ben Lakhdar, Z. 2008, Journal of Molecular Structure: THEOCHEM, 853, 18
- Huber, K. P. & Herzberg, G. 1979, Molecular Spectra and Molecular Structure IV. Constants of Diatomic Molecules, Van Nostrand, New York
- Hutson, J. M. & Green, S. 1994, MOLSCAT computer code, version 14, Collaborative Computational Project No. 6 of the Science and Engineering Research Council, United Kingdom
- Joulain, K., Falgarone, E., Des Forets, G. P., & Flower, D. 1998, A&A, 340, 241
- Knowles, P. J., Hampel, C., & Werner, H.-J. 1993, J. Chem. Phys., 99, 5219
- Knowles, P. J., Hampel, C., & Werner, H.-J. 2000, J. Chem. Phys., 112, 3106
- Maloney, P. R., Hollenbach, D. J., & Tielens, A. G. G. M. 1996, ApJ, 466, 561
- Manolopoulos, D. E. 1986, J. Chem. Phys., 85, 6425
- Nehmé, C., Le Boulrot, J., Boulanger, F., Pineau Des Forêts, G., & Gry, C. 2008, A&A, 483, 485

Table 2. Downward rate coefficients of rotational levels of CH⁺ in collision with He as a function of kinetic temperature (in units of cm³ s⁻¹).

Initial level	Final level	Rate Coefficients				
		300 K	500 K	1000 K	1500 K	2000 K
J	J'					
1	0	1.0892(-10)	1.0474(-10)	9.3755(-11)	8.6919(-11)	8.2199(-11)
2	0	5.4712(-11)	6.0895(-11)	6.8789(-11)	7.1572(-11)	7.2620(-11)
2	1	1.1448(-10)	1.1728(-10)	1.1262(-10)	1.0753(-10)	1.0347(-10)
3	0	2.1373(-11)	1.9118(-11)	1.4804(-11)	1.2486(-11)	1.1121(-11)
3	1	8.8407(-11)	1.0579(-10)	1.3046(-10)	1.4071(-10)	1.4494(-10)
3	2	7.4955(-11)	8.2783(-11)	8.9974(-11)	9.1966(-11)	9.2355(-11)
4	0	1.2349(-11)	1.6741(-11)	2.4127(-11)	2.7741(-11)	2.9365(-11)
4	1	1.8445(-11)	1.8632(-11)	1.7816(-11)	1.7104(-11)	1.6602(-11)
4	2	1.0329(-10)	1.2071(-10)	1.4877(-10)	1.6297(-10)	1.7013(-10)
4	3	4.4272(-11)	5.3386(-11)	6.6319(-11)	7.2883(-11)	7.6588(-11)
5	0	1.8893(-12)	2.1234(-12)	2.4700(-12)	2.6880(-12)	2.8346(-12)
5	1	2.6285(-11)	3.2428(-11)	4.5476(-11)	5.3674(-11)	5.8207(-11)
5	2	9.2178(-12)	1.1060(-11)	1.3795(-11)	1.5314(-11)	1.6233(-11)
5	3	9.5934(-11)	1.1444(-10)	1.4622(-10)	1.6408(-10)	1.7437(-10)
5	4	2.6196(-11)	3.4002(-11)	4.8021(-11)	5.6663(-11)	6.2226(-11)
6	0	4.5865(-12)	5.5789(-12)	8.2688(-12)	1.0468(-11)	1.1906(-11)
6	1	1.7118(-12)	2.3213(-12)	3.6910(-12)	4.7426(-12)	5.4934(-12)
6	2	2.7322(-11)	3.4211(-11)	4.9685(-11)	6.0782(-11)	6.7859(-11)
6	3	4.5014(-12)	6.5071(-12)	1.0643(-11)	1.3429(-11)	1.5279(-11)
6	4	8.6611(-11)	1.0467(-10)	1.3755(-10)	1.5779(-10)	1.7065(-10)
6	5	1.7971(-11)	2.4058(-11)	3.6692(-11)	4.5470(-11)	5.1550(-11)
7	0	2.9225(-13)	4.2016(-13)	7.6333(-13)	1.0737(-12)	1.3164(-12)
7	1	8.1105(-12)	1.0045(-11)	1.5631(-11)	2.0767(-11)	2.4497(-11)
7	2	1.5290(-12)	2.2415(-12)	4.1090(-12)	5.7047(-12)	6.9146(-12)
7	3	2.4418(-11)	3.1705(-11)	4.8123(-11)	6.0615(-11)	6.9304(-11)
7	4	4.0769(-12)	5.6780(-12)	9.7084(-12)	1.2814(-11)	1.5021(-11)
7	5	7.3617(-11)	9.2301(-11)	1.2673(-10)	1.4868(-10)	1.6326(-10)
7	6	1.5508(-11)	2.0148(-11)	3.0772(-11)	3.8740(-11)	4.4530(-11)
8	0	1.4359(-12)	1.8300(-12)	3.0413(-12)	4.3682(-12)	5.4488(-12)
8	1	9.0915(-13)	1.2019(-12)	1.9538(-12)	2.6903(-12)	3.3078(-12)
8	2	7.7361(-12)	1.0389(-11)	1.7651(-11)	2.4520(-11)	2.9880(-11)
8	3	2.3727(-12)	3.1083(-12)	5.0438(-12)	6.8186(-12)	8.2340(-12)
8	4	2.0407(-11)	2.8012(-11)	4.5156(-11)	5.8453(-11)	6.8144(-11)
8	5	5.3564(-12)	6.7877(-12)	1.0395(-11)	1.3359(-11)	1.5551(-11)
8	6	5.9379(-11)	7.8105(-11)	1.1414(-10)	1.3805(-10)	1.5436(-10)
8	7	1.6382(-11)	1.9895(-11)	2.8486(-11)	3.5245(-11)	4.0284(-11)
9	0	3.1749(-13)	4.1519(-13)	6.0967(-13)	7.9911(-13)	9.6908(-13)
9	1	2.2637(-12)	3.2040(-12)	6.0848(-12)	9.2677(-12)	1.2005(-11)
9	2	1.6464(-12)	2.1416(-12)	3.1582(-12)	4.1187(-12)	4.9529(-12)
9	3	6.3038(-12)	9.4243(-12)	1.7913(-11)	2.5792(-11)	3.2072(-11)
9	4	3.5314(-12)	4.4470(-12)	6.3778(-12)	8.1075(-12)	9.5331(-12)
9	5	1.5792(-11)	2.3335(-11)	4.0997(-11)	5.4987(-11)	6.5343(-11)
9	6	6.9032(-12)	8.4680(-12)	1.1802(-11)	1.4466(-11)	1.6473(-11)
9	7	4.6271(-11)	6.3763(-11)	9.9734(-11)	1.2494(-10)	1.4252(-10)
9	8	1.8795(-11)	2.1639(-11)	2.8624(-11)	3.4250(-11)	3.8524(-11)
10	0	3.7206(-13)	5.7888(-13)	1.2592(-12)	2.0545(-12)	2.7827(-12)
10	1	8.7732(-13)	1.2033(-12)	1.7474(-12)	2.2194(-12)	2.6452(-12)
10	2	1.9744(-12)	3.2175(-12)	7.1936(-12)	1.1441(-11)	1.5137(-11)
10	3	2.2421(-12)	3.0153(-12)	4.3132(-12)	5.3982(-12)	6.3360(-12)
10	4	4.7195(-12)	7.8986(-12)	1.7002(-11)	2.5507(-11)	3.2383(-11)
10	5	4.3451(-12)	5.6292(-12)	7.7712(-12)	9.4441(-12)	1.0795(-11)
10	6	1.1332(-11)	1.8149(-11)	3.5276(-11)	4.9542(-11)	6.0390(-11)
10	7	8.1395(-12)	1.0071(-11)	1.3538(-11)	1.6073(-11)	1.7923(-11)
10	8	3.5458(-11)	5.1093(-11)	8.5561(-11)	1.1114(-10)	1.2939(-10)
10	9	2.1861(-11)	2.4448(-11)	3.0405(-11)	3.5149(-11)	3.8707(-11)

Stäuber, P., Doty, S. D., van Dishoeck, E. F., & Benz, A. O. 2005, A&A, 440, 949

Stäuber, P., Doty, S. D., van Dishoeck, E. F., Jørgensen, J. K., & Benz, A. O. 2004, A&A, 425, 577

Sternberg, A. & Dalgarno, A. 1995, ApJS, 99, 565

Stoecklin, T. & Voronin, A. 2008, European Physical Journal D, 46, 259

Tao, F.-M. & Pan, Y.-K. 1992, J. Chem. Phys., 97, 4989

Tielens, A. G. G. M. & Hollenbach, D. 1985, ApJ, 291, 722

Werner, H.-J., Knowles, P. J., & Almöf, J., et al. 2002, MOLPRO, a package of ab initio programs, University College Cardiff Consultants Limited, see <http://www.molpro.net>

Woon, D. E. & Dunning, Jr., T. H. 1994, J. Chem. Phys., 100, 2975